International Journal of Solids and Structures 46 (2009) 1229–1239

Contents lists available at ScienceDirect

International Journal of Solids and Structures

journal homepage: www.elsevier.com/locate/ijsolstr

Bulk-stress effects in double contacts of similar elastic materials

N. Sundaram *, T.N. Farris

School of Aeronautics and Astronautics, Purdue University, 701 W. Stadium Ave., West Lafayette, IN 47907-2045, United States

ARTICLE INFO

Article history:
Received 3 July 2008
Received in revised form 2 October 2008
Available online 7 November 2008

Keywords:
Contact
Singular integrals
Half-space
Friction
Numerical methods
Integral equation

ABSTRACT

The effects of a remote applied stress on double contacts of similar elastic materials are examined using a numerical method based on Cauchy singular integral equations (SIE). In contrast to single contacts, the space of possible shear configurations is very rich. In many cases, the partial slip problem does not have a contact equivalent. An equation based on displacement continuity is derived to relate the stick-zone extents for any shear configuration; this equation is essential for the solution of general partial slip problems involving two stick-zones. A shear configuration map that shows the types of partial slip solution that occur for various shear load-remote bulk-stress combinations is obtained for biquadratic indenters. Lastly, it is shown that it is possible to predict the shear configuration in some cases for double cylindrical indenters.

1. Introduction

Two-dimensional contact mechanics is a well-established area of mechanics with extensive analytical and numerical work to determine contact area, pressure and shear tractions under partial slip conditions. For a review, see the paper by Barber et al. (2000). Assuming that the two contacting bodies can be treated as half-spaces allows the formulation of the contact problem as a pair of Cauchy singular integral equations (SIEs) for the pressure and shear tractions. The equations are uncoupled if the two bodies are similar. The effect of a remote bulk stress on *single* cylindrical contacts was first investigated by Nowell et al. (1987) and Nowell and Hills (1987) to analyze their fretting fatigue experiments. In the former work, they obtained a closed form solution for the case when the sign of slip is the same in both slip zones. In the latter, they used a numerical technique developed by Erdogan et al. (1973) to solve a Cauchy SIE for the case when the sign of slip is opposite in the two slip zones. Two interacting contacts occur in a number of situations. For instance, post-failure examination of fretting fatigue specimens occasionally shows two macroscopic contact patches; the cause is usually a machining artifact or surface treatment. Prior work by Sundaram and Farris (2008) focused on developing a SIE-based numerical method to obtain contact extents and pressure tractions for such contacts, and then solving the partial slip problem using equivalence between the pressure and shear problems. (A detailed discussion on the equivalence technique is available in Ciavarella, 1998a, Ciavarella, 1998b and Jaeger, 1997.)

However, the presence of a remote bulk-stress in addition to a shear load complicates the partial slip double contact problem. First, the number of possible shear configurations is much larger when a remote bulk-stress is applied. Second, only a subset of partial slip problems with applied bulk-stress have contact equivalents which allow a solution using the method discussed in the authors' prior work. In particular, a new relationship between the ends of the stick-zones which is independent of an equivalent contact is required to yield a unique solution. This relationship, used in combination with a numerical method to invert a Cauchy SIE on two disconnected segments of the x-axis, forms the basis for solving various types of partial slip problems in double contacts.

2. Governing equations for similar contacts

When two bodies are brought into contact (see Fig. 1), the vertical separation or gap function $h(x)$ between them may be written as (Barber, 2002)

$$h(x) = h_0(x) - v_1 + v_2 - C_0 - C_1 x \quad \forall x, \tag{1}$$

where v_1 and v_2 are the vertical *surface* displacements of the two bodies, $h_0(x)$ is the initial gap function (or the undeformed indenter profile in case of indentation of a flat body), C_1 is the term associated with rigid-body rotation and C_0 with rigid-body translation. It is assumed that the rotation C_1 is small.

By definition, the gap function has to be zero inside the contact, so that

$$v_1 - v_2 = h_0(x) - C_0 - C_1 x \tag{2}$$

* Corresponding author.
E-mail addresses: nsundara@purdue.edu (N. Sundaram), farrist@purdue.edu (T.N. Farris).

0020-7683/$ - see front matter © 2008 Elsevier Ltd. All rights reserved.
doi:10.1016/j.ijsolstr.2008.10.030

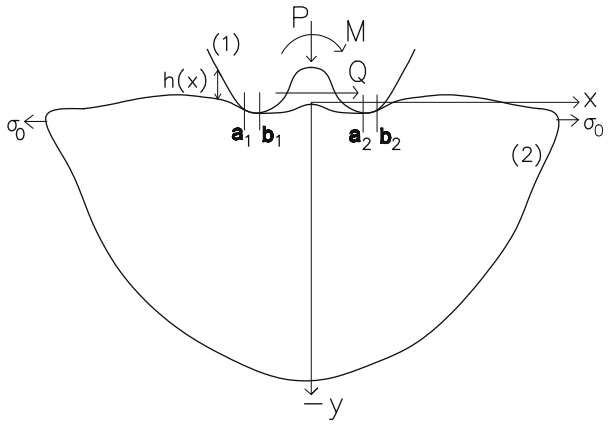

Fig. 1. Double contact configuration.

within the contact. Using Flamant's solution for point-loads on a half-space as a Green's function, this equation can be rewritten as a SIE

$$\frac{dh_0(x)}{dx} - C_1 = A\int_L \frac{p(s)}{x-s}ds \quad \forall x \in L, \tag{3}$$

where L is the set of points in contact, $p(x)$ the pressure traction and A is a term encapsulating elastic behavior in plane strain, $A = 4(1-\nu^2)/\pi E$ for similar, isotropic material contact. For similar materials, the pressure equation is unaffected by the presence of friction. For so-called incomplete contacts, L is *a priori* unknown. The pressure traction must satisfy the equilibrium equations

$$\int_L p(x)dx = P, \tag{4}$$

$$\int_L xp(x)dx = M, \tag{5}$$

where P and M *are,* respectively, the applied normal load and moment. Positive pressure is considered compressive in the nomenclature used above. The contact area L must be determined such that the pair of inequalities

$$p(x) > 0 \quad \forall x \in L, \tag{6}$$

$$h(x) > 0 \quad \forall x \notin L, \tag{7}$$

is satisfied. Here, $h(x)$ is the gap function. These conditions simply state that the contact pressure must be compressive inside the contact and there is no interpenetration outside the contact (Barber, 2002). For two contacts

$$\frac{dh_0(x)}{dx} - C_1 = A\int_{L_1} \frac{p_1(s)}{x-s}ds + A\int_{L_2} \frac{p_2(s)}{x-s}ds \quad \forall x \in \{L = L_1 \cup L_2\}, \tag{8}$$

where L_1 and L_2 are the contact patches and the $p_1(x), p_2(x)$ are the pressure traction in each patch. The resultant conditions for the pressure and moment are

$$\int_{L_1} p_1(x)dx + \int_{L_2} p_2(x)dx = P, \tag{9}$$

$$\int_{L_1} xp_1(x)dx + \int_{L_2} xp_2(x)dx = M. \tag{10}$$

In the discussion that follows, the notation a_k, b_k will be used for the left and right ends of the kth contact, i.e., $L_k = (a_k, b_k)$, where $k = 1, 2$. It will also be assumed that the pressure tractions $p_1(x), p_2(x)$ contact extents and rotation C_1 are obtained using the numerical method discussed by Sundaram and Farris (2008) in prior work.

If friction is present, the contact can transmit shear tractions in addition to normal tractions. Usually, contacts can be divided into two different types of regions: in the stick (or adhesion) zones, there is no relative motion between the two bodies and in the slip zones, the two bodies experience relative motion. Then, in the stick-zones, the governing equation for the shear-traction $q(x)$ is the following SIE:

$$\left.\frac{ds(x)}{dx}\right|_{k-1} = A\int_L \frac{q^{(k)}(s)}{x-s}ds - \frac{\sigma_0^{(k)}(1-\nu^2)}{E} \quad \forall x \in S, \tag{11}$$

where S is the set of all points in stick, $\sigma_0^{(k)}$ is a remote bulk-stress applied to body 2, '$s(x)$' is the slip function and the superscript 'k' represents the kth step of loading. Also, in the stick-zones, the maximum value of shear traction is limited as per the Amontons–Coulomb friction model

$$|q(x)| < \mu p(x), \tag{12}$$

where μ is the coefficient of friction. In the slip zones

$$q(x) = sign\left(\frac{ds(x,t)}{dt}\right)\mu p(x). \tag{13}$$

In a quasi-static approach, the time variable does not appear explicitly, so the gradient in the equation above is reduced to a difference as follows:

$$q(x) = sign(s^{(k)}(x) - s^{(k-1)}(x))\mu p(x). \tag{14}$$

Considering the shear traction as two different functions $q_1(x)$ and $q_2(x)$ in the two contacts, Eq. (11) can be written as

$$\left.\frac{ds(x)}{dx}\right|_{k-1} = A\int_{L_1} \frac{q_1^{(k)}(s)}{x-s}ds + A\int_{L_2} \frac{q_2^{(k)}(s)}{x-s}ds - \frac{\sigma_0(1-\nu^2)}{E} \quad \forall\, x \in \{S = S_1 \cup S_2\}. \tag{15}$$

The stick regions in the two contacts, S_1 and S_2 are unknown *a priori*. For equilibrium

$$\int_{L_1} q_1^{(k)}(x)dx + \int_{L_2} q_2^{(k)}(x)dx = Q. \tag{16}$$

In subsequent discussions, the ends of the stick-zones in the contacts will be denoted by $a_1^q, b_1^q, a_2^q, b_2^q$ where $S_1 = (a_1^q, b_1^q)$ and $S_2 = (a_2^q, b_2^q)$. It is well known that the presence of friction introduces path-dependence in contact problems, i.e., for the most gen-

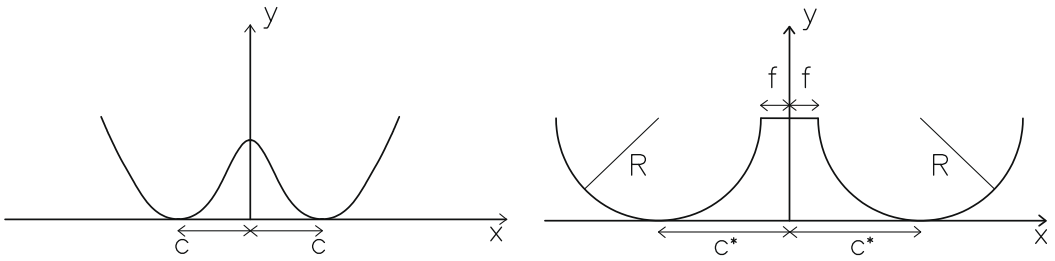

Fig. 2. Profiles of the biquadratic indenter (left) and the double cylindrical indenter (right).

Table 1
Possible shear configurations in partial slip.

Type	Stick-zones	Sign of $q(x)$ in slip zones	Equivalent contact?	Type	Stick-zones	Sign of $q(x)$ in slip zones	Equivalent contact?
3-1	2	++/+−	N	3-0	1	*L*+/++	Y
	2	−+/++	N		1	*L*−/−−	Y
	2	+−/− −	N		1	++/*L*+	Y
	2	−+/++	N		1	− −/*L*−	Y
2-1a	1	*L*+/+−	N	2-1s	1	*L*+/− −	N
	1	*L*−/−+	N		1-	− −/*L*+	N
	1	−+/*L*+	N		1	++/*L*−	N
	1	+−/*L*−	N		1	− −/*L*+	N
2-2	2	++/− −	N	4-0	2	++/++	Y
	2	− −/++	N		2	− −/− −	Y

eral types of load paths in the P, M, Q, σ_0 space it is essential to solve the shear traction problem incrementally and update the slip function $s(x)$ at the end of each increment.

While the solution techniques discussed in this work are easily extended to general load paths, the load path of interest in so-called Cattaneo–Mindlin type problems is one which involves applying a normal load P, and moment M concurrently in the first step and then, while these are kept constant, applying a shear load and bulk-stress Q, σ_0 in the second load-step, followed by a possible reversal of these loads in the third load-step. Such load paths are important, for example, in the design of fretting fatigue experiments. It is possible to represent a general 'R' step load path in a concise way by specifying a set of load vectors of the form $[P] = (P_1, P_2, \ldots, P_R)$, $[M] = (M_1, M_2, \ldots, M_R)$, $[Q] = (Q_1, Q_2, \ldots, Q_R)$, $[\sigma_0] = (\sigma_{0,1}, \sigma_{0,2}, \ldots, \sigma_{0,R})$. The subscripts denote the load-step. When square brackets are used, it will be understood to refer to a load vector rather than the load in a single step. For example, the 'fretting' type loads just described above may be denoted by the load vectors $[P] = (P, P, P)$, $[M] = (M, M, M)$, $[Q] = (0, +Q, -Q)$ and $[\sigma_0] = (0, +\sigma_0, -\sigma_0)$. The strain $g_0 = \sigma_0(1 - \nu^2)/E$ may also be specified instead of the bulk-stress.

3. Possible shear traction configurations

Based on the combination of signs of shear traction in the slip zones, it is possible to identify various 'shear configurations'. Shear configurations differ from each other based on the signs of shear in the slip zones and the number of stick-zones.[1] Different shear configurations occur depending on the applied loads. The problem of deciding *which* shear configuration occurs for a particular set of loads will be set aside for the time being. Table (1) summarizes possible shear configurations in double contacts, and also introduces a simple, short-hand notation for them. For example, consider '3-1' shear. Here '3-1' means three slip zones with shear of one sign and one of the opposite sign. There are two stick-zones in such a configuration. The table also shows that there are different '3-1' shear configurations based on the combinations of signs of shear in the slip zones; each is written specifying the sign of shear starting with the leftmost slip zone and progressing rightward. For example, '++/+−' means the left contact has positive $q(x)$ in both its slip zones, and the right contact has positive $q(x)$ in its left slip zone and negative $q(x)$ in its right slip zone. The / sign separates the left and right contacts. An '*L*' is used to indicate that a (particular) contact is in sliding, with the sign of shear in that contact specified after the '*L*'. For example, − − /*L*− indicates that the left contact has negative signs of shear in both slip zones, and the right contact is in full sliding.

[1] In similar contacts, the end of a stick-zone may coincide with the end of a contact. These 'boundary' cases are best considered separately.

The question of whether such a table is exhaustive for double contacts is an open one, even when the load path is restricted to $[P] = (P, P)$, $[M] = (M, M)$, $[Q] = (0, Q)$, $[\sigma_0] = (0, \sigma_0)$. However, the techniques used in the present work may be easily extended to handle *any* other double contact partial slip configuration (whether or not it has a contact equivalent) as long as it involves no more than two stick-zones.

4. Numerical method

To solve the partial slip problem in double contacts resulting in two stick-zones, it is essential to have a method to invert a Cauchy SIE defined on two non-intersecting segments of the x-axis. Such a method is discussed in prior work by Sundaram and Farris (2008) for the normal contact problem in double contacts; the method is re-derived here (in a slightly modified form) for the sake of completeness. First of all, the stick-zone equation (15) for all partial slip problems involving two stick-zones has to be converted into a form suitable for analysis. This is achieved by substituting for the unknown shear tractions $q_1^{(k)}(x), q_2^{(k)}(x)$ by the sum of known functions of the pressure traction and new unknowns which go to zero at the ends of the stick-zone. In addition, each of the new unknown functions is zero outside the stick-zones. The exact substitution to be used to achieve this re-formulation is different for different shear configurations and will be detailed later. Assume that after the re-formulation, the shear traction SIE has the following generic form:

$$\frac{df}{dx} = K \int_{S_1} \frac{w_1(s)}{x - s} ds + K \int_{S_2} \frac{w_2(s)}{x - s} ds - g_0 \quad \forall x \in S_1 \cup S_2. \tag{17}$$

Here, w_1 and w_2, the unknown functions, are bounded. The function w_1 goes to zero at either end of the stick-zone S_1 and is zero everywhere outside it. Similarly, the function w_2 goes to zero at either end of the stick-zone S_2 and is zero everywhere outside it, i.e.,

$$w_1(x) = 0 \quad \forall x \notin S_1, \tag{18}$$

$$w_2(x) = 0 \quad \forall x \notin S_2. \tag{19}$$

The function df/dx is a known, Hölder continuous function of x and the K, g_0 are known constants. It must be emphasized here that the SIE (17) does not, in general, represent that of a contact pressure problem. For instance, it is possible for the unknown functions w_1, w_2 to cross zero a finite number of times. For arbitrarily specified domains S_1 and S_2, this SIE does not, in general, have solutions that are bounded at all ends (Muskhelishvili, 1992). In other words, the bounded solutions are embedded at discrete locations in the space spanned by the extent variables $min(S_1), max(S_1), min(S_2), max(S_2)$. This is problematic because the physically correct stick-zone extents are unknown *a priori*, and have to be determined by searching this space iteratively. However, solutions that are *unbounded* do exist for arbitrary S_1 and S_2. With this in mind, square-root form singularities are introduced in the unknowns as follows:

$$w_1(x) = w_0^I(x) + \phi_1\sqrt{\frac{b_1^q - x}{x - a_1^q}} \quad \forall x \in S_1, \tag{20}$$

$$w_2(x) = w_0^{II}(x) + \phi_2\sqrt{\frac{x - a_2^q}{b_2^q - x}} \quad \forall x \in S_2. \tag{21}$$

Here, $w_0^I(x)$ and $w_0^{II}(x)$ are functions that are bounded everywhere, and the (unknown) constants ϕ_1 and ϕ_2 are coefficients of the singular terms. A search for bounded solutions $w_1(x), w_2(x)$ is equivalent to searching for those points in the $min(S_1), max(S_1)$, $min(S_2), max(S_2)$ space where ϕ_1 and ϕ_2 go to zero. Substituting these expressions in Eq. (17) leads to

$$\frac{1}{K}\frac{df(x)}{dx} + g_0 = \sum_{m=1}^{2}\int_{S_m}\frac{w_0^m(s)ds}{x-s} + \int_{S_1}\phi_1\sqrt{\frac{b_1^q - s}{s - a_1^q}}\frac{ds}{x-s} + \int_{S_2}\phi_2\sqrt{\frac{s - a_2^q}{b_2^q - s}}\frac{ds}{x-s}. \tag{22}$$

To solve the equation numerically, the domains S_1 and S_2 are discretized by division into $N_I + 1$ and $N_{II} + 1$ node points, respectively. The SIE (22) is enforced at N_I and N_{II} collocation points x_k^I and x_k^{II} in the regions S_1 and S_2, respectively. The node points and collocation points have to be as far away from each other as possible for accurate evaluation of the integrals, and for this purpose each collocation point is set equidistant from its neighboring node points, i.e., $x_k = 0.5 * (s_{k+1} + s_k)$. Analytically, integrating the terms containing the coefficients ϕ and discretizing the 'x' domain as indicated lead to the following sets of equations:

$$\frac{1}{K}\left(\frac{df(x_k^I)}{dx} + g_0\right) = \sum_{m=1}^{2}\int_{S_m}\frac{w_0^m(s)ds}{x_k^I - s} + \pi\phi_1 - \pi\phi_2\left(1 - \left(\frac{a_2^q - x_k^I}{b_2^q - x_k^I}\right)^{1/2}\right), \quad k = 1\ldots N_I, \tag{23}$$

$$\frac{1}{K}\left(\frac{df(x_k^{II})}{dx} + g_0\right) = \sum_{m=1}^{2}\int_{S_m}\frac{w_0^m(s)ds}{x_k^{II} - s} - \pi\phi_2 + \pi\phi_1\left(1 - \left(\frac{x_k^{II} - b_1^q}{x_k^{II} - a_1^q}\right)^{1/2}\right), \quad k = 1\ldots N_{II}. \tag{24}$$

Next, the bounded functions w_0^m are expressed as piecewise linear functions of their unknown nodal values as follows:

$$w_0^m(s) = w_0^m(s_i) + \frac{s - s_i}{\Delta s_m}\left(w_0^m(s_{i+1}) - w_0^m(s_i)\right), \quad m = 1, 2. \tag{25}$$

Here, Δs_m is the nodal spacing in the mth stick-zone and the nodal location s_i in the mth stick-zone is given by

$$s_i^m = a_m^q + (i-1)\Delta s^m = a_m^q + (i-1)\frac{b_m^q - a_m^q}{N_m}, \quad m = 1, 2. \tag{26}$$

Define

$$J_0(x; m, n) = \int_{S_m}\frac{w_0^m(s)ds}{x_k^n - s} \approx \sum_{i=1}^{N_m}\int_{s_i}^{s_{i+1}}\frac{w_0^m(s)ds}{x_k^n - s}, \quad m \neq n. \tag{27}$$

This set of integrals is non-singular when $m \neq n$. Replacing w_0^m by nodal quantities using Eq. (25) and carrying out the integrations inside the sum

$$J_0(x; m, n) = \sum_{i=1}^{N_m}\left(w_{0,i}^m L + \frac{w_{0,i+1}^m - w_{0,i}^m}{\Delta s_m}\left(-\Delta s_m - (s_i^m - x_k^n)L\right)\right), \quad m \neq n, \tag{28}$$

where $w_{0,i}^m \equiv w_0^m(s_i)$ and $L = \log((s_i^m - x_k^n)/(s_{i+1}^m - x_k^n))$. The special case $m = n$ contains one singular integral inside the sum, which must be evaluated as a Cauchy principal value. In this case

$$J_0(x; m, m) = \sum_{\substack{i=1 \\ i \neq k}}^{N_m}\left(w_{0,i}^m L + \frac{w_{0,i+1}^m - w_{0,i}^m}{\Delta s_m}\left(-\Delta s_m - (s_i^m - x_k^m)L\right)\right) + w_{0,k}^m - w_{0,k+1}^m. \tag{29}$$

After carrying out these operations, a linear system of equations is obtained. It has $(N_I + 1) + (N_{II} + 1) = N + 2$ unknown nodal quantities and two unknown singularity coefficients giving a total number of $N + 4$ unknowns. Enforcing the SIE at the $N_I + N_{II} = N$ collocation points gives N equations. In addition, the condition that the functions w_1, w_2 should go to zero at the ends a_m^q, b_m^q of each stick-zone yields an additional four equations $w_0(a_m^q) = 0, w_0(b_m^q) = 0$ for $m = 1, 2$. It is now possible to invert this linear system for a set of specified trial stick-zone end values a_m^q and b_m^q during an iterative search to find the stick-zone extents.

5. Continuity equation for arbitrary shear configurations

When two stick-zones are present, the four stick-zone ends are not independent; a relationship may be obtained between them based on considerations of continuity of the tangential displacement, u. Consider a problem involving 'k' loading steps for which the shear traction has been obtained up to and including step $k-1$, i.e., the slip function at the end of step $k-1$, s_{k-1} is known everywhere. Now, assume that after step 'k' partial slip conditions exist. By definition, there should be no relative slip in the stick-zones at the end of step 'k', so that

$$s_k(b_1^q) = s_{k-1}(b_1^q), \tag{30}$$

$$s_k(a_2^q) = s_{k-1}(a_2^q). \tag{31}$$

Let u_I and u_{II} be the surface tangential displacements of the upper and lower bodies, respectively, at the end of step 'k'. Then, given the displacement at an arbitrary reference point x_0, it is clear that

$$u_{I,II}(x) = u_{I,II}(x_0) + \int_{x_0}^{x}\left(\frac{du_{I,II}(x)}{dx}\right)dx \quad \forall x. \tag{32}$$

These equations are applicable for any pair (x, x_0) assuming piecewise continuous displacement gradients. Subtracting

$$u_I(x) - u_{II}(x) = u_I(x_0) - u_{II}(x_0) + \int_{x_0}^{x}\left(\frac{du_I(x)}{dx} - \frac{du_{II}(x)}{dx}\right)dx \quad \forall x. \tag{33}$$

Using the definition of the slip function $s_k \equiv u_I(x) - u_{II}(x)$ and choosing $x_0 = b_1^q, x = a_2^q$ in Eq. (33)

$$s_k(a_2^q) = s_k(b_1^q) + \int_{b_1^q}^{a_2^q}\left(\frac{du_I(x)}{dx} - \frac{du_{II}(x)}{dx}\right)dx \quad \forall x. \tag{34}$$

Using Eqs. (30) and (31) in the above

$$s_{k-1}(a_2^q) - s_{k-1}(b_1^q) = \int_{b_1^q}^{a_2^q}\left(\frac{du_I(x)}{dx} - \frac{du_{II}(x)}{dx}\right)dx \quad \forall x. \tag{35}$$

Notice that the left-hand side is a known quantity. The next step is to express the right-hand side in terms of the tractions in step 'k'. For elastic half-spaces (Barber, 2002)

$$\frac{du_I}{dx} = \frac{\kappa + 1}{4\pi G}\int_L\frac{q^{(k)}(s)}{x-s}ds + \frac{\kappa - 1}{4G}p^{(k)}(x), \tag{36}$$

$$\frac{du_{II}}{dx} = -\frac{\kappa + 1}{4\pi G}\int_L\frac{q^{(k)}(s)}{x-s}ds + \frac{\kappa - 1}{4G}p^{(k)}(x) + g_0^{(k)}, \tag{37}$$

where G is the shear modulus and g_0^k is related to the remote bulk-stress applied in the kth step as

$$g_0^{(k)} = \frac{\sigma_0^{(k)}(1-\nu^2)}{E}. \tag{38}$$

It appears in only one of the equations because the upper body is not subjected to remote bulk loads (see Fig. 1). Subtracting (37) from (36) and substituting into Eq. (35)

$$s_{k-1}(a_2^q) - s_{k-1}(b_1^q) = \int_{b_1^q}^{a_2^q} \left[\frac{\kappa+1}{2\pi G}\int_L \frac{q^{(k)}(s)}{x-s}ds\right]dx - \int_{b_1^q}^{a_2^q} g_0^{(k)}dx. \tag{39}$$

Recognizing that $A = (\kappa+1)/2\pi G$ and integrating

$$s_{k-1}(a_2^q) - s_{k-1}(b_1^q) + g_0^{(k)}(a_2^q - b_1^q) = A\int_{b_1^q}^{a_2^q}\left(\int_L \frac{q^{(k)}(s)}{x-s}ds\right)dx. \tag{40}$$

Eq. (40) is a very general statement about the relationship between the four stick-zone ends (a_1^q and b_2^q appear explicitly when the inner integral is written out completely). Note that it makes no assumptions about the nature of the shear tractions. An arbitrarily chosen set of a_1^q, b_1^q, a_2^q and b_2^q will not, in general, satisfy Eq. (40) above and it is possible to define a new function V_s:

$$V_s(a_1^q, b_1^q, a_2^q, b_2^q) \equiv s_{k-1}(a_2^q) - s_{k-1}(b_1^q) + g_0^{(k)}(a_2^q - b_1^q) - A\int_{b_1^q}^{a_2^q}\left(\int_L \frac{q^{(k)}(s)}{x-s}ds\right)dx, \tag{41}$$

where the physically correct solution satisfies $V_s = 0$. If the partial slip problem has a contact equivalent, it is easily verified by substituting for $q(x)$ that Eq. (40) reduces to the following:

$$h_0^*(b_1^q) - h_0^*(a_2^q) + C_1^* a_2^q - C_1^* b_1^q + \int_{b_1^q}^{a_2^q}\left(\frac{dv^*}{dx}\right)dx = 0. \tag{42}$$

The asterisks denote quantities in the equivalent pressure problem. This equation represents the condition that the ends of contact of a rigid indenter indenting a half-space (with modulus $E/2$ and no friction) can only undergo rigid-body motions (Sundaram and Farris, 2008).

6. Indenter profiles

Two simple indenter profiles (see Fig. 2) are considered to study bulk-stress effects in double contacts. The biquadratic indenter is defined by a fourth degree polynomial as follows (Gladwell, 1980):

$$y(x) = \frac{x^4}{8Rc^2} - \frac{x^2}{4R} + \frac{c^2}{8R} = \frac{(x^2-c^2)^2}{8Rc^2}. \tag{43}$$

Here, 'c' is half the distance between the minima of the biquadratic indenter. The indenter has minima at $\pm(c,0)$ and a maximum at $(0,0)$.

The double cylinder is a connected pair of cylinders defined in the following way:

$$y(x) = \begin{cases} \frac{(x+c^*)^2}{2R}, & x < -f, \\ k_0, & -f \leqslant x \leqslant f, \\ \frac{(x-c^*)^2}{2R}, & x > f. \end{cases} \tag{44}$$

Both cylinders are of radius R and the centers of the cylinders are at $(-c^*, R)$ and (c^*, R), respectively. The constant $k_0 > 0$ is chosen so that the profile is C_0 continuous at $\pm f$ and any value $0 < f < c^*$ may be chosen for f as long as the contact patches do not extend into the region $(-f, f)$ for the applied loads P, M. The minima of this profile are located at $\pm(c^*, 0)$. Note that this profile is locally parabolic unlike the biquadratic indenter.

The normalization parameters used for the biquadratic indenter are the merge load[2] $F^* = c^2/4AR$ and the clockwise moment M^* at which one of the contacts 'lifts-off' *for a given value of P*. The normal load normalization parameter used for the cylindrical indenter is $F^* = (c^*)^2/2AR$, and M^* is defined as in the case of the biquadratic indenter. Applied bulk-stresses are normalized by μp^{max}, where p^{max} is the peak pressure. All future references to these normalization constants should be interpreted in this way.

7. 3-1 Partial slip problem

When the applied bulk-stress σ_0^k exceeds a certain threshold, a 3-1 type shear configuration is obtained. Consider ++/+− as an example of 3-1 type shear. It has shear of opposite signs in the right contact. The SIE for the shear traction is, as before,

$$\left.\frac{ds(x)}{dx}\right|_{k-1} = A\int_{L_1}\frac{q_1^k(s)}{x-s}ds + A\int_{L_2}\frac{q_2^k(s)}{x-s}ds - g_0^k \quad \forall x \in \{S = S_1 \cup S_2\} \tag{45}$$

in the stick-zones, where g_0^k is the strain. In this case, the substitutions to be used to convert the shear SIE to the form in Eq. (17) are

$$q_1^k(x) = \mu p_1(x) - q_1^*(x), \tag{46}$$

$$q_2^k(x) = \mu f_2^+(x) - q_2^*(x), \tag{47}$$

where $p_1(x), p_2(x)$ are the (known) pressure tractions in the two contacts, $q_1^*(x), q_2^*(x)$ are functions that are non-zero only in the respective stick-zones of the two contacts and $f_2^+(x)$ is (following Farris, 1992 for single contacts)

$$f_2^+(x) = \begin{cases} p_2(x), & a_2 < x < a_2^q, \\ p_2(a_2^q) + \left(\frac{p_2(b_2^q) - p_2(a_2^q)}{b_2^q - a_2^q}\right)(x - a_2^q), & a_2^q < x < b_2^q, \\ -p_2(x), & b_2^q < x < b_2. \end{cases} \tag{48}$$

Substituting Eqs. (46) and (47) in Eq. (45) and rearranging

$$\int_{S_1}\frac{q_1^*(s)}{x-s}ds + \int_{S_2}\frac{q_2^*(s)}{x-s}ds = \frac{1}{A}\left(-\left.\frac{ds(x)}{dx}\right|_{k-1} - g_0^k\right) + \mu\int_{L_1}\frac{p_1(s)}{x-s}ds + \mu\int_{L_2}\frac{f_2^+(s)}{x-s}ds \quad \forall x \in S. \tag{49}$$

For a set of specified stick-zone ends, the right-hand side of this equation is a known function of x.[3] The SIE may now be inverted using the numerical method discussed previously. For a set of arbitrary trial stick-zone ends, the result contains singularities, i.e. ϕ_1, ϕ_2 are non-zero and these ultimately have to go to zero. Further, the equilibrium equation to be satisfied is now

$$Q^* \equiv \int_{S_1} q_1^*(x)dx + \int_{S_2} q_2^*(x)dx = \mu\int_{L_1} p_1(x)dx + \mu\int_{L_2} f_2^+(x)dx - Q. \tag{50}$$

In addition to the equilibrium condition, $\phi_1 = 0$ and $\phi_2 = 0$, the continuity condition $V_s = 0$ (Eq. (41)) also has to be satisfied, giving four conditions in all for the four unknown stick-zone ends. Starting from a trial solution vector $\{X\} = \{a_1^q, b_1^q, a_2^q, b_2^q\}^T$, the updated solution vector is obtained using a 4D Newton–Raphson scheme as

$$\{X_{i+1}\} = \{X_i\} + \left[\frac{\partial(Q^*, \phi_1, \phi_2, V_s)}{\partial(a_1^q, b_1^q, a_2^q, b_2^q)}\right]^{-1}\{R_i\}, \tag{51}$$

[2] The applied normal load at which the two contact patches merge into one, at zero applied moment.

[3] Accurate evaluation of the RHS needs care because, depending on the location of x, one or the other of these integrals only exists as a Cauchy principal value.

where R_i is the vector of residuals after 'i' iterations (indicated by the subscript 'i')

$$R_i = \{-(Q_i^* - \mu(P_1 + F_2) - Q), -\phi_{1i}, -\phi_{2i}, -V_i\}^T. \quad (52)$$

The first residual represents the error in satisfying equilibrium equation (50). Q_i^* is obtained by integrating over the non-singular part of the functions q_1^*, q_2^*. The derivatives in the Jacobian matrix are evaluated numerically by calculating function values at neighboring points, e.g.,

$$\frac{\partial V_s}{\partial a_1^q} \approx \frac{V_s(a_1^q + \Delta a_1^q, b_1^q, a_2^q, b_2^q) - V_s(a_1^q, b_1^q, a_2^q, b_2^q)}{\Delta a_1^q}. \quad (53)$$

Here, Δa_1^q is a small change in a_1^q. The iteration process is continued till the residuals are less than certain pre-specified tolerances. It is possible to proceed in a similar way for the +−/−−, −−/−+ and −+/++ shear cases.

Consider the biquadratic indenter with the normal load and moment vectors given by $[P] = 0.755F^*(1,1,1)$ and $M = (0,0,0)$. Two different load paths that cause 3-1 type shears are considered. For path-I, $[Q] = \mu P(0.0, +0.2, -0.2), [\sigma_0]/\mu p^{max} = 0.5(0, +1, -1)$ and for path-II, $[Q] = \mu P(0.0, -0.3, +0.3), [\sigma_0]/\mu p^{max} = 0.5(0, +1, -1)$. Fig. 3 shows normalized shear tractions obtained using SIE for these cases; the top plot for path-I and the bottom plot for path-II. All tractions are normalized by μ times the peak pressure p^{max} in this plot as well as subsequent ones and the x-axis is normalized by the apparent contact half-size ('a'). The dotted lines in this plot (and subsequent ones) indicate full sliding; the regions where the $\pm\mu * p(x)$ lines coincide with the normalized shear tractions correspond to slip zones. There is one stick-zone in each contact as before, but one of the slip zones has a sign of shear different from the other three. The SIE solutions took about 30 s each on a desktop PC with 850 collocation points.

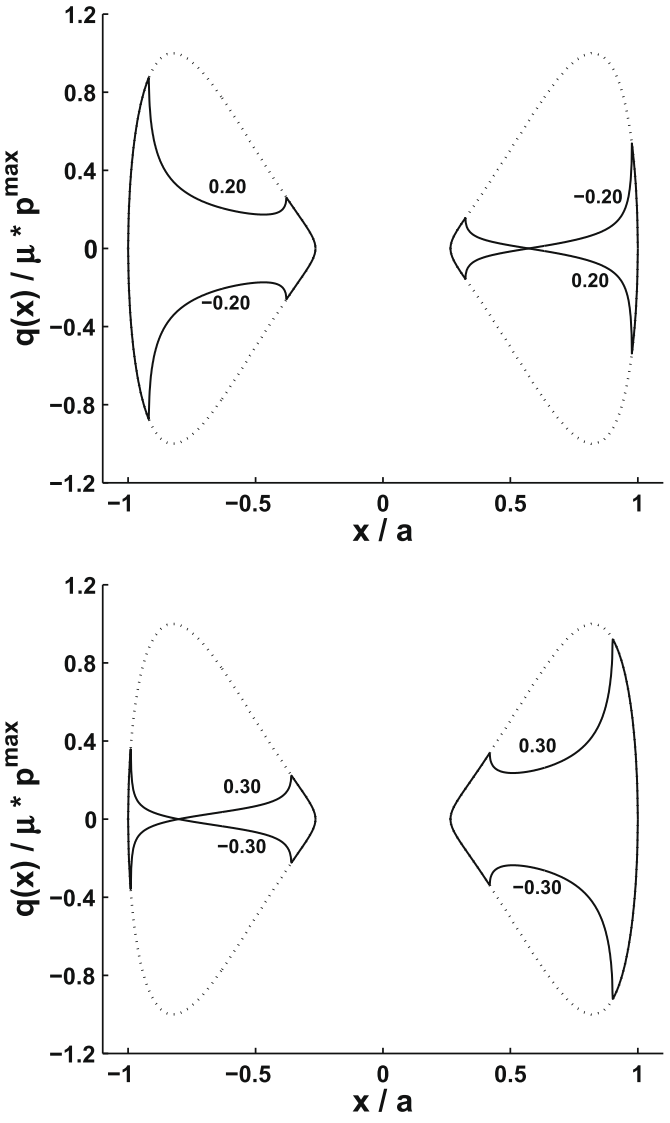

Fig. 3. SIE normalized shear tractions $q(x)/\mu p^{max}$ of the 3-1 type for the biquadratic indenter. In the top figure, a shear load $Q = 0.2\mu P$ and $\sigma_0/\mu p^{max} = 0.5$ are applied in step 2 and then fully reversed in load-step 3. In the bottom figure, a shear load $Q = -0.3\mu P$ and $\sigma_0/\mu p^{max} = 0.5$ are applied in step 2 and then fully reversed in load-step 3. The value of applied $Q/\mu P$ is indicated next to each line.

8. 4-0 Partial slip problem

In this case, the magnitude of the remote bulk-stress σ_0^k is small enough compared to the applied shear load magnitude Q so that the sign of the shear tractions in all four slip zones is the same. For example, in the case $sign(\Delta Q) \equiv sign(Q_k - Q_{k-1}) > 0$, where '$k$' denotes the load-step, the shear tractions q_1, q_2 are rewritten in terms of the pressure tractions and corrective shear functions $q_1^*(x), q_2^*(x)$ using the following substitutions to obtain an equation of the form, Eq. (17):

$$q_1^k(x) = \mu p_1(x) - q_1^*(x), \quad (54)$$

$$q_2^k(x) = \mu p_2(x) - q_2^*(x). \quad (55)$$

Each corrective shear function is non-zero only in the stick-zone of that particular contact. Using this substitution and the pressure equation, the following SIE is obtained:

$$\left[\mu \frac{dh_0(x)}{dx} - \frac{ds(x)}{dx}\bigg|_{k-1}\right] - [\mu C_1 + g_0^k] = A\int_{S_1} \frac{q_1^*(s)}{x-s} ds + A\int_{S_2} \frac{q_2^*(s)}{x-s} ds \quad \forall x \in S. \quad (56)$$

By integrating Eqs. (54) and (55), the equilibrium condition to be satisfied is $Q^* = \mu P - Q$. In this case, the solution of the partial slip problem is equivalent to solving a double contact problem with the rotation specified. The equivalent rotation is $C_2 = \mu * C_1 + g_0^k$ and is known beforehand, unlike the normal contact problem where the moment M is specified instead. Q^* may be interpreted as the normal load applied on the equivalent contact, and V_s is now the error in satisfying either Eq. (40) or (42). Again, the four conditions to be satisfied are the equilibrium condition, $\phi_1 = 0$, $\phi_2 = 0$ and $V_s = 0$ and a 4D Newton–Raphson scheme may be used as in the 3-1 case.

Consider the biquadratic indenter with the following 'fretting-type' load path. $[P] = 0.755F^*(1,1,1,1)$, $M = 0.1M^*(1,1,1,1)$, $[Q] = \mu P(0.0, +0.5, 0.0, -0.5)$ and stress $[\sigma_0]/\mu p^{max} = 0.24(0, +1, 0, -1)$. Step 3 is an intermediate load point in shear reversal. The first plot in Fig. 4 shows normalized shear tractions obtained using SIE with the applied value of $Q/\mu P$ indicated on the plot. There is one stick-zone in each contact, and all four slip zones have the same sign of shear, namely ++/++ and then −−/−− on reversal. The 4-step SIE solution using 850 collocation points took about 25 s on a desktop PC. The second plot in Fig. 4 shows the shear tractions obtained in steps 2-4 for the double cylinder subjected to the load path $[P] = 0.675F^*(1,1,1,1)$, $M = 0.16M^*(1,1,1,1)$, $[Q] = \mu P(0.0, +0.5, 0.0, -0.5)$ and $[\sigma_0]/\mu p^{max} = 0.45(0, +1, 0, -1)$.

9. 2-2 Partial slip problem

This configuration occurs for large σ_0^k for relatively small Q. Consider the ++/−− configuration as an example. The shear tractions are rewritten using the substitutions

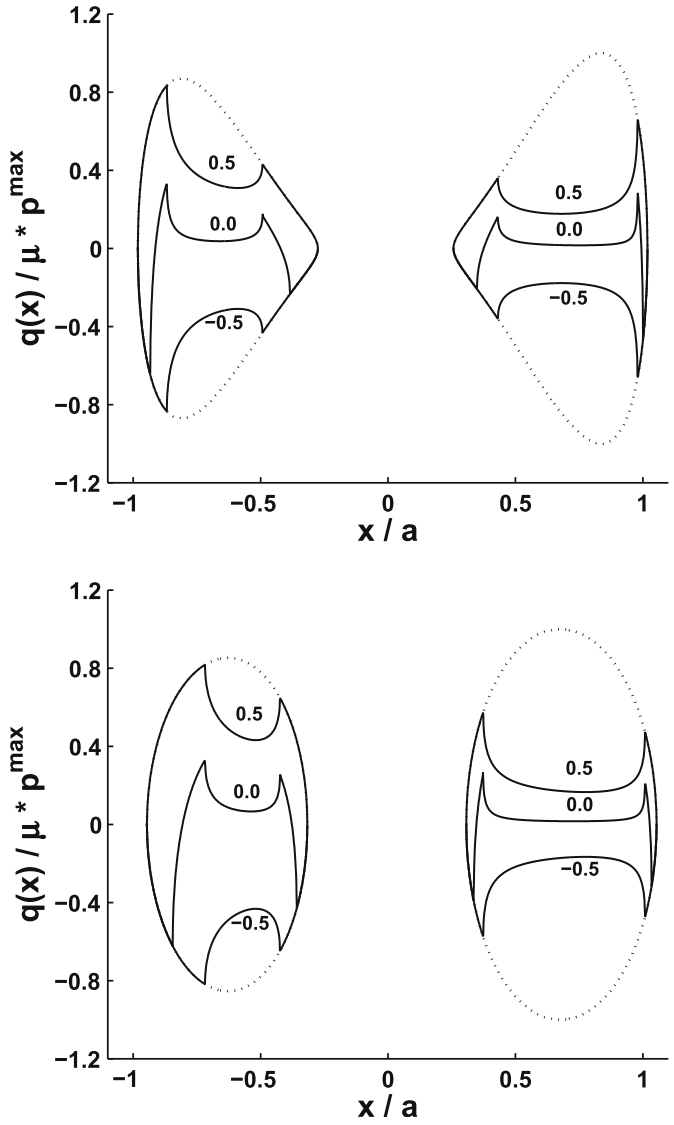

Fig. 4. SIE normalized shear tractions $q(x)/\mu p^{max}$ of the 4-0 type for the biquadratic indenter (top) and double cylinder (bottom) with applied Q, σ_0 in load-steps 2, partially reversed Q, σ_0 in step 3 and fully reversed Q, σ_0 in step 4. The value of applied $Q/\mu P$ is indicated next to each line.

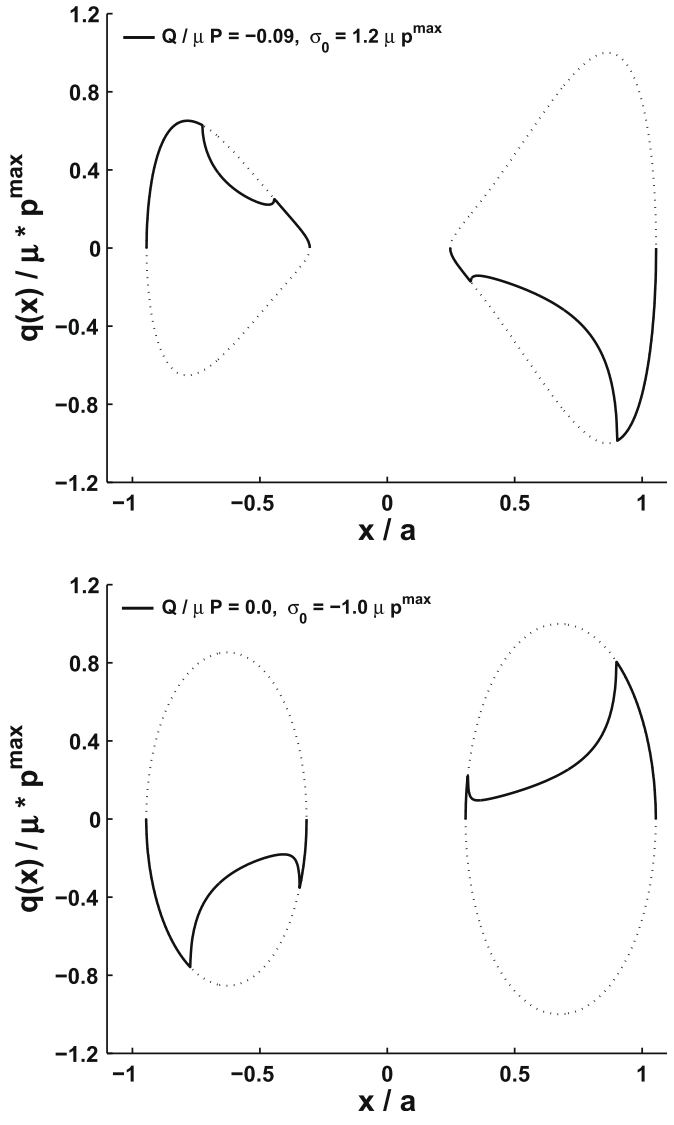

Fig. 5. SIE normalized shear tractions $q(x)/\mu p^{max}$ of the 2-2 type for the biquadratic indenter (top) and double cylinder (bottom) in load-step 2. For the biquadratic indenter, $Q/\mu P$=-0.09, $\sigma_0/\mu p^{max} = 1.2$. For the double cylinder, $Q = 0$, $\sigma_0/\mu p^{max} = -1.0$.

$$q_1^k(x) = \mu p_1(x) - q_1^*(x), \tag{57}$$

$$q_2^k(x) = -\mu p_2(x) + q_2^*(x) = -\mu p_2(x) - q_f(x), \tag{58}$$

to convert the shear SIE into the generic form, Eq. (17). Then,

$$\int_{S_1} \frac{q_1^*(s)}{x-s} ds + \int_{S_2} \frac{q_f^*(s)}{x-s} ds = \frac{1}{A}\left(-\left.\frac{ds(x)}{dx}\right|_{prev} - g_0\right) + \mu \int_{L_1} \frac{p_1(s)}{x-s} ds - \mu \int_{L_2} \frac{p_2(s)}{x-s} ds \quad \forall x \in S. \tag{59}$$

In this case, the right-hand side is a known function of x. The equilibrium condition to be satisfied is

$$\int_{S_1} q_1^*(x)dx + \int_{S_2} q_f^*(x)dx = \mu \int_{L_1} p_1(x)dx - \mu \int_{L_2} p_2(x)dx - Q. \tag{60}$$

Again, a 4D Newton–Raphson scheme may be used to obtain the stick-zone ends to satisfy $\phi_{1,2} = 0, V_s = 0$ and the equilibrium equation above. The shear tractions obtained using SIE for such a shear configuration are shown in Fig. 5 for both the biquadratic indenter (top) and double cylinder (bottom). For the biquadratic indenter, $[P] = 0.755F^*(1,1)$, $M = 0.3M^*(1,1)$, $[Q] = \mu P(0.0, -0.09)$ and $[\sigma_0]/\mu p^{max} = 1.2(0, +1)$. The load path for the double cylinder is $[P] = 0.675F^*(1,1)$, $M = 0.16M^*(1,1)$, $[Q] = (0,0)$ and $[\sigma_0]/\mu p^{max} = (0, -1)$. Notice that in both cases, the signs of shear in the slip zones of the left and right contacts are opposite to each other.

10. 3-0 Partial slip problem

Consider the sub-type $L+/++$. Since the left contact is in sliding, a transformation of the type

$$q_1^k(x) = \mu p_1(x), \tag{61}$$

$$q_2^k(x) = \mu p_2(x) - q_2^*(x), \tag{62}$$

is used. There is only one corrective shear traction in this case, and using this substitution and the pressure equation, an equivalent contact SIE is obtained as follows:

$$\left[\mu \frac{dh_0(x)}{dx} - \left.\frac{ds(x)}{dx}\right|_{k-1}\right] - \left[\mu C_1 + g_0^k\right] = A \int_{S_2} \frac{q_2^*(s)}{x-s} ds \quad \forall x \in S, \tag{63}$$

i.e., using equivalence, this problem reduces to an equivalent *single* contact problem, with equivalent pressure $\mu P - Q$. The equivalent pressure over this single contact may be determined analytically for both the bi-cylinder and the biquadratic indenter for load paths of the type $[P] = (P, P)$, $[M] = (M, M)$, $[Q] = (0, Q)$, $[\sigma_0] = (0, \sigma_0)$. For the double-cylinder, the equivalent pressure is of the standard elliptical form

$$q^*(x) = \frac{\sqrt{(e_q + a_q - x)(x - e_q + a_q)}}{\pi A R_q}, \tag{64}$$

where $R_q = R/\mu$, and the stick-zone half-length a_q and eccentricity e_q are given by

$$a_q = \sqrt{2AR_qP_{eq}}, \quad e_q = c^* + R_q(\mu C_1 + g_0). \tag{65}$$

For the biquadratic indenter, the single contact equivalent pressure is

$$q^*(x) = \frac{\sqrt{a_q^2 - (e_q - x)^2}(a_q^2 + 2(x^2 + e_q x + e_q^2 - c^2))}{4\pi A c^2 R_q}, \tag{66}$$

where $R_q = R/\mu$ and a_q, e_q satisfy the following algebraic equations:

$$\frac{e_q(3a_q^2 - 2c^2 + 2e_q^2)}{4c^2 R_q} = \mu C_1 + g_0, \tag{67}$$

$$\frac{a_q^2(3a_q^2 - 4c^2 + 12e_q^2)}{16Ac^2 R_q} = \mu P - Q. \tag{68}$$

It is possible to proceed in a similar way for $++/L+, --/L-$ and $L-/--$. For general slip histories and/or profiles, it is not possible to obtain an analytical solution for the equivalent pressure; however, any of the well-known numerical techniques to solve single contact SIEs may be used instead (e.g. Hills and Nowell (1994)).

The top plot in Fig. 6 shows the shear tractions obtained when the biquadratic indenter is subjected to the load path $[P] = 0.755F^*(1,1,1,1)$, $M = 0.2M^*(1,1,1,1)$, $[Q] = \mu P(0.0, +0.7, 0.0, -0.7)$ and $[\sigma_0]/\mu p^{max} = 0.5(0, +1, 0, -1)$. Steps 3 and 4 are obtained using the SIE technique, while $q^*(x)$ in step 2 is obtained analytically using Eq. (66). 3-0 type shear occurs in steps 2 and 4 (with the left contact in full sliding); the intermediate step 3 shows a 4-0 type traction. The bottom plot in Fig. 6 shows the shear tractions obtained for a double cylinder subjected to the loading $[P] = 0.675F^*(1,1,1,1)$, $M = 0.45M^*(-1,-1,-1,-1)$, $[Q] = \mu P(0.0, +0.65, 0.0, -0.65)$ and $[\sigma_0]/\mu p^{max} = 0.55(0, -1, 0, +1)$. The right contact is now in sliding in steps 2 and 4.

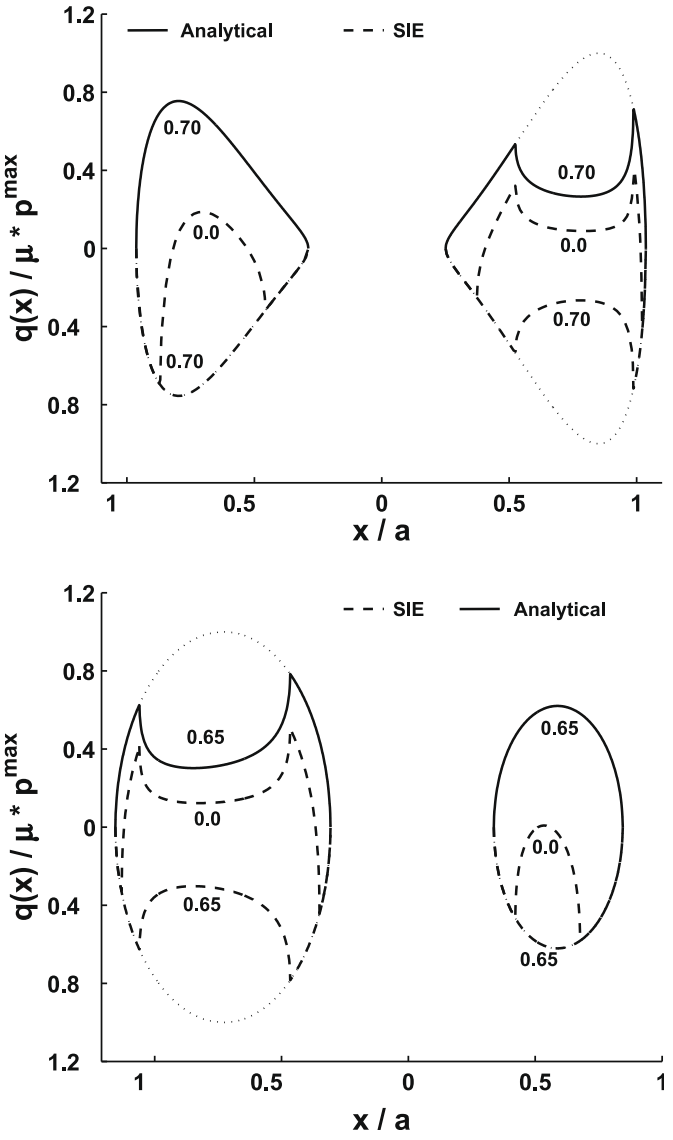

Fig. 6. Analytical (solid lines) and SIE (dashed lines) normalized shear tractions $q(x)/\mu p^{max}$ in steps 2-4 for the biquadratic indenter (top) and double cylinder (bottom) subjected to three-quarters of a fretting cycle. For the biquadratic indenter, $|Q|/\mu P$=0.7, $|\sigma_0|/\mu p^{max} = 0.5$ in steps 2 and 4. When the loads are partially reversed to 0 in step 3, a 4-0 type shear configuration is obtained. For the double cylinder, $|Q|/\mu P = 0.65$, $|\sigma_0|/\mu p^{max} = 0.55$ in steps 2 and 4 with partially reversed loads in step 3.

11. 2-1 Partial slip problem

In this case, it is again possible to convert the problem to one on a single region. While the problem is not an equivalent contact problem, a numerical method similar to those used to solve single contact partial slip problems with shear of opposite signs in the two slip zones may be used for type 2-1a (Nowell and Hills (1987)). Other single contact methods may be used for type 2-1s partial slip problems. Again, only the results are presented here.

Consider the biquadratic indenter with load vectors given by $[P] = 0.755F^*(1,1), [M] = 0.1M^*(1,1), [Q] = \mu P(0.0, -0.5), [\sigma_0]/\mu p^{max} = (0, -1.0)$. The top plot in Fig. 7 shows normalized shear tractions obtained using SIE for this case. The left contact is in full sliding and the right contact has slip zones with opposite signs of shear. The bottom plot in Fig. 7 shows the shear tractions for the double cylinder with load vectors $[P] = 0.675F^*(1,1)$, $[M] = 0.16M^*(1,1)$, $[Q] = \mu P(0.0, 0.5), [\sigma_0]/\mu p^{max} = (0, 1.05)$. The SIE solutions took about 25 s each on a desktop PC with 850 collocation points.

12. Solution check

Once a candidate solution is obtained using any of the techniques discussed above, it is essential to test that it is physically accurate, i.e. the sign of slip satisfies Eq. (14) and the stick-zone inequality equation (12) holds. If the solution fails the slip test equation (14) anywhere, it usually implies the presence of a stick-zone in a region assumed to be slipping. This occurs, for instance, when the 3-0 solver is used in a situation where the physically correct solution is of type 4-0.

13. Biquadratic indenter shear configuration map

The space of shear configurations that occur for various load combinations may be visualized conveniently using a shear configuration map. This is a map generated at a fixed value of P and M,

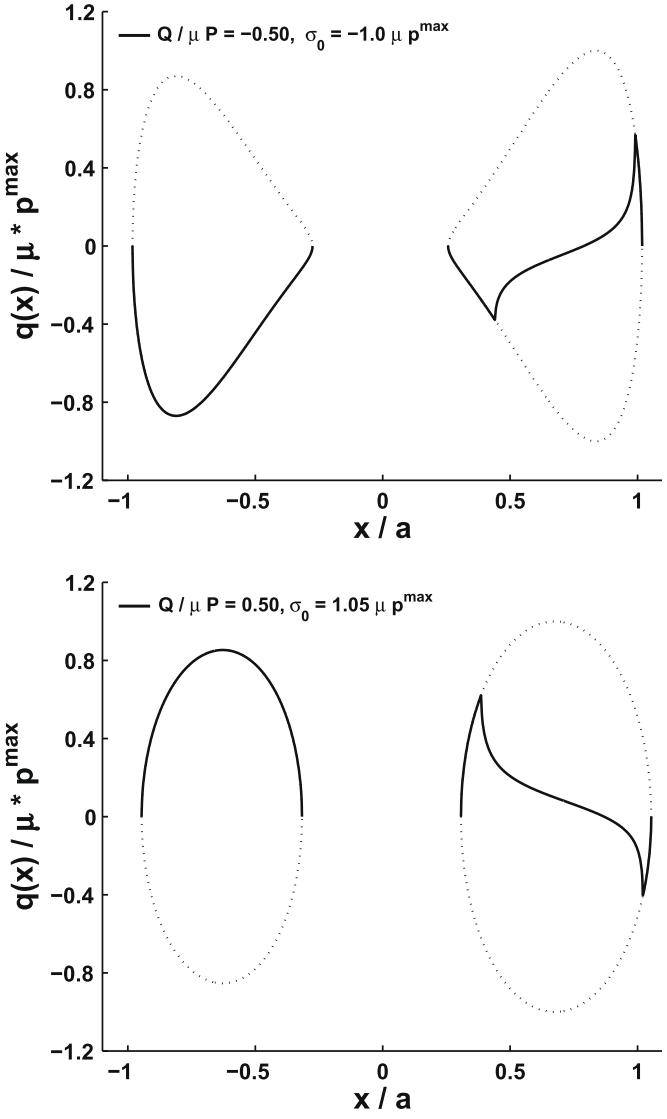

Fig. 7. SIE normalized shear tractions $q(x)/\mu p^{max}$ of the 2-1a type for a biquadratic indenter (top) and double cylinder (bottom) in load-step 2. For the biquadratic indenter, $Q/\mu P = -0.5$, $\sigma_0/\mu p^{max} = -1.0$. The left contact is in full sliding ($q_1(x) = -\mu p_1(x)$). For the double cylinder, $Q/\mu P = 0.5$, $\sigma_0/\mu p^{max} = 1.05$.

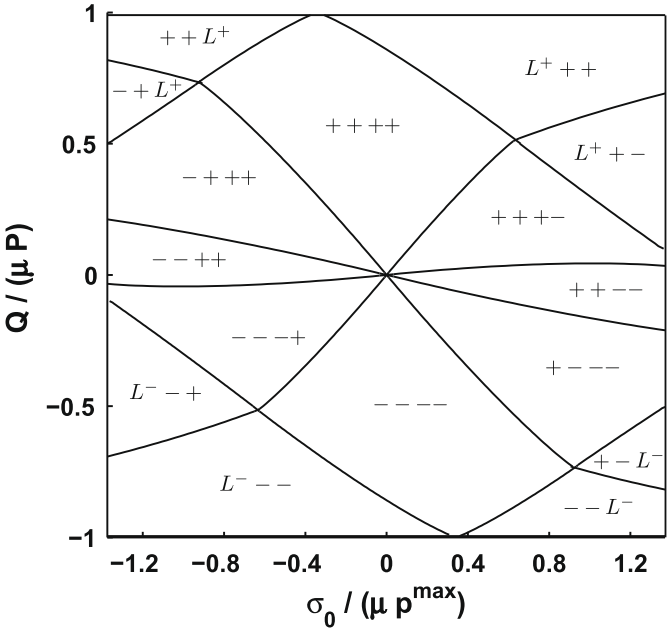

Fig. 8. Shear configuration map for the biquadratic indenter.

Table 2
Shear configuration map boundaries.

Boundary separates	Type	Solution type
4-0/3-1	Stick	Equivalent double contact
4-0/3-0	Sliding	Equivalent single contact
3-1/2-2	Stick	Double contact partial slip
3-1/2-1a	Sliding	Single contact partial slip
3-0/2-1a	Stick	Equivalent single contact

with Q, and σ_0 varied. As usual P, M are applied first and then Q, σ_0. The map is generated by solving for the boundaries; it is possible to do so analytically in a few cases only (see Appendix for some results for double cylinders). In general, determining each boundary involves the numerical solution of a special problem in which one of Q, σ_0 is treated as an unknown (in contrast to partial slip problems in which both are specified). An additional equation is provided by the special conditions prevailing along the boundary. For 'stick type' boundaries, one of the stick-zone ends coincides with a contact end. For 'sliding type' boundaries, one of the contacts goes from partial slip to full sliding. By varying the known parameter (either Q or σ_0), a sequence of solutions is obtained that corresponds to the boundary.

Fig. 8 shows a normalized shear configuration map for the biquadratic indenter for applied normal load $P = 0.754F^*$ and moment $M/M^* = 0.2025$. Q varies from $-\mu P$ to μP, and the normalized stress $\sigma_0/\mu p^{max}$, from -1.35 to 1.35. Each region is labeled with a shear configuration. The effect of the bulk-stress is immediately evident: the 4-0 and 3-0 shear configurations are the only ones that can occur if no bulk-stress is applied. The effect of the moment is to break the symmetry (a map at $M = 0$ would be symmetric about both x and y axes) and favor sliding in one or the other contact depending on the signs of applied Q and σ_0. However, there is symmetry about the origin, which is a result of using a symmetric indenter profile. The solid horizontal lines at ± 1 represent full sliding in both contacts.

A summary of the types of boundaries found in Fig. 8 and the solution schemes used to obtain them is provided in Table 2.

14. Discussion

The solutions obtained using the SIE technique for various shear configurations for both indenter types show very good agreement when compared with FEM results.

It is useful to briefly consider the influence of profile geometry on the shear tractions; this is best characterized by using the dimensionless ratio c/R (or c^*/R). A higher value of c/R indicates weaker interaction between the two contacts. Further, the interaction between the two contact patches is weaker for double-cylinders than biquadratic punches when $c/R = c^*/R$. This is because the curvature of the biquadratic indenter is about $1/R$ in the neighborhood of $\pm c$ and smaller than that when $|x| < c$. This 'flattening' effect leads to larger contact patches for the same normal loads (more specifically a smaller inner contact-end to contact-end distance), which means more interaction between the patches. The weakened interaction at larger c/R is best demonstrated by considering a simplified situation for the double cylinder: in the absence of applied moment M and bulk-stress σ_0, the tractions are very well approximated at large values of c^*/R by locally Hertzian single

contact tractions for pressure and Cattaneo–Mindlin single-contact shear with P, Q divided equally between the two contacts. The peak shear traction is also lower than in the case when c^*/R is smaller. It is difficult to make such any such predictions in the presence of significant bulk-stresses.

It is also worth comparing the method used in this work with the quadratic programing approach found in Kalker (1971) and Nowell and Dai (1998) to solve other contact problems. In such an approach, no distinction is made between regions of stick and slip; instead, a unified metric is used to characterize the error in violating the friction laws and this metric minimized (subject to a mixture of equality and inequality contraints) using standard optimization techniques. In contrast to this global approach, using the present semi-analytical approach the friction law is obeyed locally (and exactly) by the final solution. In addition, distinguishing regions of stick and slip allows Eq. (40) to be enforced explicitly, which is important from the perspective of displacement continuity. The optimization approach, on the other hand, has the advantage of eliminating the need for separate consideration of individual shear configurations.

15. Conclusions

The effects of a remote applied stress on double contacts of similar elastic materials were examined using a fast numerical method based on SIEs. An equation based on displacement continuity was derived to relate the stick-zone ends for any shear configuration. Numerical results were obtained for both biquadratic and double-cylindrical indenters. A map of the shear configurations that occur for various shear load-remote bulk-stress combinations was obtained for biquadratic indenters.

Acknowledgements

This work is supported partially by DARPA on a subcontract to GE Aircraft Engines. The authors also thank the anonymous reviewers for their many helpful suggestions.

Appendix. Analytical results for double cylinders

In the case of double cylindrical indenters, it is sometimes possible to predict which shear configuration occurs for a given Q, σ_0 combination (i.e. *some* of the boundaries in the shear configuration map may be obtained analytically). In particular, consider the case of the boundary between 4-0 shear regions and the 3-0 shear regions. Here, there is an exact correspondence between the problem of determining the moment M^{crit} for a given applied load P at which one contact of a double-cylindrical indenter 'lifts-off' resulting in a single contact and the problem of determining, for a given shear load Q, the bulk-stress σ_0^{crit} (or strain g_0^{crit}) at which one contact goes into full sliding.

Consider the indentation of a half-space by a single cylindrical indenter of similar elastic properties, with the difference that the minimum of the cylinder is located off-axis at a location $(c^*, 0)$ where $c^* > 0$. Let the contact patch be (a_1, b_1).

The resulting pressure traction $p(x)$ on applying a normal load P is still elliptical, but is offset from the origin by a distance 'e' where $e > 0$.

$$p(x) = \frac{\sqrt{(b_1 - x)(x - a_1)}}{\pi AR} \tag{69}$$

and the contact extents, eccentricity and rotation are given by

$$a = \sqrt{2ARP} \quad \text{where } a = \frac{b_1 - a_1}{2}, \quad e = \frac{b_1 + a_1}{2}, \quad \text{and } C_1 = \frac{e - c^*}{R}. \tag{70}$$

The presence of a load P acting eccentric to the global coordinate system may be interpreted as an applied clockwise moment $M = Pe$.[4]

Now, consider this cylinder to be coincident with the right-hand portion of the (symmetric) double-cylindrical indenter with inter-minimal separation $c = 2c^*$. Apply loads P, M applied to the *double cylinder* such that the physical solution has two contacts. Using the single contact solution above will result in gap inequality violations (i.e., overclosures) in a region roughly corresponding to where the second contact should exist. For any applied normal load P, there is a certain value M_{crit}, corresponding to 'lift-off', where this region degenerates into a single point at some location $x^* < -f$ where $h(x^*) = 0$. If $h(x)$ is a smooth function in this neighborhood, the single point of contact also indicates that the gap function has a minimum at this location, so that at 'lift-off', the following conditions apply:

$$h(x^*) = 0, \quad \frac{dh(x^*)}{dx} = 0. \tag{71}$$

The slope of the gap function is given everywhere by

$$\frac{dh}{dx} = \frac{dh_0}{dx} - A\int_{a_1}^{b_1} \frac{p(s)}{x - s} ds - C_1 \quad \forall x, \tag{72}$$

where dh_0/dx is the initial gap function. Substituting Eq. (69) into this equation and integrating, the condition that the slope of the gap function goes to zero at a location $x^* < -f$ is

$$\frac{x^* + c^*}{R} + \frac{1}{R}\left(e - \sqrt{(a_1 - x^*)(b_1 - x^*)} - x^*\right) - C_1 = 0. \tag{73}$$

Replacing a_1, b_1 by e, a and substituting the value of C_1 gives

$$\sqrt{(e - a - x^*)(e + a - x^*)} = c. \tag{74}$$

The gap function is obtained as

$$h(a_1) - h(x^*) = \int_{x^*}^{a_1} \frac{dh(x)}{dx} dx. \tag{75}$$

Performing the integration and simplifying, the condition $h(x^*) = 0$ may be rewritten as

$$a^2 \log\left[\frac{a}{e - x^* + c}\right] = -c(e + x^*). \tag{76}$$

It is possible to solve Eqs. (74) and (76) explicitly for e, x^* by introducing a new variable $y = e - x^*$. Then, Eq. (74) becomes

$$\sqrt{(y - a)(y + a)} = c, \tag{77}$$

whence $y = \sqrt{a^2 + c^2}$. The positive root of y is chosen to obtain a minimum. Substituting y in Eq. (76), solving for x^*, using $e = y + x^*$ and recalling that $M = Pe$ gives an explicit solution for the critical or 'lift-off' moment M_{crit} for a double cylindrical indenter for any applied load P.[5]

$$M_{crit} = P\left(\frac{\sqrt{a^2 + c^2}}{2} - \frac{a^2}{2c}\log\left[\frac{a}{\sqrt{a^2 + c^2} + c}\right]\right), \tag{78}$$

where $a = \sqrt{2ARP}$ and $A = 4(1 - \nu^2)/\pi E$. Since the profile is symmetric, there is also an anticlockwise moment $-M_{crit}$ where the right contact of the double cylinder lifts-off.

For the equivalent problem, the equivalent pressure $P_{eq} = \mu P - Q$ and $C_2 = \mu C_1 + g_0^k$. The equivalent cylindrical profile $\mu\, dh_0/dx$ has a radius $R_q = R/\mu$. The relation between the eccentricity and rotation is given by Eq. (70)

[4] Note that the cylinder does not support a resultant moment *locally* and the pressure traction in Eq. (69) is symmetric about $x = e$.

[5] Of course, this analysis assumes that the applied load P is such that no part of the region $[-f, f]$ comes into contact.

$$C_2 = \frac{e_q - c^*}{R_q}. \tag{79}$$

Substituting for $e_q = M_{crit}/P$ from Eq. (78) leads to the following value of critical strain:

$$g_0^{crit,+} = \frac{1}{2R_q}\left(\sqrt{a_q^2 + c^2} - \frac{a_q^2}{c}\log\left[\frac{a_q}{\sqrt{a_q^2 + c^2} + c}\right] - c\right) - \mu C_1, \tag{80}$$

where $a_q = \sqrt{2AR_qP_{eq}}$. There is also a second value $g_0^{crit,-}$ at which the stick-zone in the right contact disappears, i.e.

$$g_0^{crit,-} = -g_0^{crit,+} - 2\mu C_1. \tag{81}$$

References

Barber, J., 2002. Elasticity Solid Mechanics and its Applications, 2nd ed. Kluwer Academic Publishers, The Netherlands.

Barber, J., Ciavarella, M., 2000. Contact mechanics. International Journal of Solids and Structures 37, 29–43. August.

Ciavarella, M., 1998a. The generalized cattaneo partial slip plane contact problem. I – Theory. International Journal of Solids and Structures 35 (18), 2349–2362.

Ciavarella, M., 1998b. The generalized cattaneo partial slip plane contact problem. II – Examples. International Journal of Solids and Structures 35 (18), 2363–2378.

Erdogan, F., Gupta, G., Cook, T.S., 1973. Numerical solution of singular integral equations. In: Sih, G. (Ed.), Methods of Analysis and Solutions of Crack Problems. Noordhoff, Leyden, pp. 368–425.

Farris, T., 1992. Mechanics of fretting fatigue tests of contacting dissimilar elastic bodies. Tribology Transactions 35, 346–352.

Gladwell, G., 1980. Contact Problems in the Classical Theory of Elasticity. Monographs and Textbooks on Mechanics of Solids and Fluids. Sijthoff and Noordhoff, The Netherlands.

Hills, D., Nowell, D., 1994. Mechanics of Fretting Fatigue. Vol. 30 of Solid Mechanics and its Applications. Kluwer Academic Publishers, The Netherlands.

Jaeger, 1997. Half-planes without coupling under contact loading. Archive of Applied Mechanics 67, 247–259.

Muskhelishvili, N., 1992. Singular Integral Equations Dover Books on Mathematics. Dover, The United States of America.

Nowell, D., Hills, D.A., 1987. Mechanics of fretting fatigue tests. International Journal of Mechanical Science 29 (5), 355–365.

Nowell, D., Hills, D., O'Connor, J., 1987. An analysis of fretting fatigue. In: Proceedings of The International Conference on Tribology. I.Mech.E., London.

Sundaram, N., Farris, T., 2008. Numerical analysis of double contacts of similar elastic materials. ASME Journal of Applied Mechanics 75 (6), 0610171–0610179.

Kalker, J.J., 1971. A minimum principle for the law of dry friction with application to elastic cylinders in rolling contact (part I). ASME Journal of Applied Mechanics 38, 875–880.

Nowell, D., Dai, D.N., 1998. Analysis of surface tractions in complex fretting cycles using quadratic programming. ASME Journal of Tribology 120, 744–749.